

# Local Pressure Difference over a NACA0018 Airfoil with Cavity Using Acoustic Forcing

W.F.J. Olsman,\* M.M.E. van Osch,† A. Hirschberg,‡ R.R. Trieling,§ and J.F.H. Willems¶  
*Eindhoven University of Technology, Eindhoven, 5600 MB, The Netherlands*

S.J. Hulshoff||

*Delft University of Technology, Delft, 2600 GB, The Netherlands*

The influence of a cavity on the steady and unsteady local pressure difference over a NACA0018 airfoil is investigated experimentally and compared to numerical calculations. In the experiments a new experimental method is used, which allows Strouhal numbers at which self-sustained oscillation of cavity flows is expected. The airfoil is fixed to the wind tunnel and the flow is modulated transversally to the main flow by an acoustic standing wave generated by loudspeakers. The objective is to obtain insight into the dynamical behavior of an airfoil with a cavity by comparison of experimental data to the results of a two-dimensional numerical Euler code. In the Strouhal range from 2.5 up to 10, based on the semi-chord, both experiment and numerical simulation do not show a strong effect of the cavity on the dynamical response of the wing. This response is dominated by the added mass of the wing.

## Nomenclature

$U$	Velocity, m/s
$\rho$	Density, kg/m <sup>3</sup>
$f$	Frequency, Hz
$\omega$	Angular frequency $2\pi f$ , rad/s
$c$	Chord length, m
$b$	Half chord $c/2$ , m
$i$	Imaginary unit
$p$	Pressure, Pa
$W$	Cavity width, m
$k_b$	Strouhal number $\frac{\omega b}{U_\infty}$
$k_b$	Strouhal number $\frac{\omega W}{U_\infty}$
$\hat{v}$	Velocity of plate, m/s
$v'$	Acoustic velocity in y-direction, m/s
$\theta$	Angle in transformed plane if Joukowski mapping, rad
$\alpha$	Angle of attack, deg.

### Subscript

$u$	Indicates an unsteady variable
$\infty$	Free stream conditions

\*PhD. student, Applied physics, w.f.j.olsman@tue.nl.

†M.Sc. Student, Mechanical Engineering.

‡Professor, Applied physics.

§Lecturer, Applied physics.

¶Technician, Applied physics.

||Assistant professor, Faculty of Aerospace Engineering, Delft.

## I. Introduction

The work presented in this paper was carried out within the framework of the European (EU) project VortexCell2050.<sup>1</sup> The goal of this project is to design a relatively thick wing without massive vortex shedding. In order to prevent downstream vortex shedding, the vortex is trapped in a cavity in the vicinity of the wing at all times.

The objective of the present paper is to gain insight into the steady and unsteady behavior of an airfoil with a cavity by experimental measurements, and the comparison of these experiments with a standard airfoil without cavity, thin airfoil theory and numerical Euler simulations. It is well known that unsteady forces can cause a wing to flutter. Knowledge of the unsteady forces on a wing is therefore crucial for successful wing design. Flutter for conventional wings has been thoroughly investigated and documented.<sup>2,3</sup> A wing with cavity, however, may show very different dynamical behaviour which is not captured by the conventional theories. In this paper we will focus on the plunging motion of an airfoil. The dynamical behaviour of an airfoil with a cavity will be investigated using local pressure measurements, which are compared to a numerical model.

The results of the pressure measurements on an airfoil with cavity are compared to those obtained on a standard airfoil without cavity. We also compare these experimental data with the predictions of linear potential theory<sup>2</sup> and two-dimensional Euler simulations. The front edge of the cavity is sharp and although the separation at the front edge of the cavity is expected to display strong three-dimensional effects, a uniform forcing will tend to synchronize the separation which will render the flow quasi two-dimensional and justifies the use of a two-dimensional flow solver. Comparison of the experimental data with Euler calculations might result in knowledge about the importance of viscosity in this particular problem.

The conventional method for dynamic measurements on an airfoil is to mount the airfoil on a rig, which is displaced with respect to the main flow by a mechanical system.<sup>4,5</sup> In this paper we will use a different method. The airfoil is fixed to the wind tunnel walls and the flow is modulated. This avoids the need of a complex mechanical system to displace the airfoil.

A lot of research has been performed on rectangular cavities in plane walls. In contrast, not much literature is available for the case of a cavity placed in an airfoil. Note that in the literature concerning cavities the Strouhal number is usually defined as  $fW/U$ , with  $W$  the opening of the cavity,  $U$  the free stream velocity and  $f$  the frequency in Hz. In this paper, the Strouhal number is defined as  $k_b = \frac{\omega b}{U}$ , with  $b$  the half chord of the airfoil and  $\omega$  the angular frequency in rad/s, the subscript  $b$  denotes that the half chord was used as a reference length. This corresponds to the reduced-frequency parameter used in the flutter literature. From the literature about cavities in flat walls it is known that a cavity can display a shear layer instability mode when the Strouhal number,  $k_W = \frac{\omega W}{U}$ , is of order 3, where  $W$  is the opening of the cavity.<sup>6</sup> The cavity may also give rise to a cavity wake mode,<sup>7</sup> although this mode is rarely observed in experiments.

The opening of the cavity  $W$  in the experiments is about 1/5 of the chord length  $2b$ . This implies that in order to have a Strouhal number  $k_W = 3$  for the cavity, the Strouhal number with respect to the half chord,  $k_b$  should be 7.8. At such high Strouhal numbers the forces on the airfoil are dominated by the added mass of the airfoil. Using the conventional measurement method, where the airfoil is displaced with respect to the flow, it will be difficult to reach such a high Strouhal number. Therefore in this paper a different method will be applied.

First the experimental method will be described, then the results of measurements and numerical simulations for a standard NACA0018 airfoil are presented as a validation of the measurement method. In the last section the results for a NACA0018 airfoil with a cavity will be discussed.

## II. Experimental method

The test facility is a low-speed wind tunnel with a square test section of 500 mm  $\times$  500 mm, and a length of 1000 mm. The walls of the test section are manufactured from plywood with a wall thickness of 24 mm. The wind tunnel walls are reinforced with wooden ribs of 10 cm height and 3.6 mm width, to reduce the effects of wall vibrations. The maximum velocity in the test section is about 67 m/s, which corresponds to a Mach number of 0.19 at room temperature. The velocity is determined by measuring the pressure difference between the settling chamber and the test section with a MU DIGITAL manometer, neglecting the velocity in the settling chamber. The velocity is determined with an accuracy of 0.2%. The turbulence intensity is less than 0.2% in an empty test section. In each of the two opposite side walls of the test section is a circular

hole with a diameter of 200 mm, which is covered with fabric. On the outside of the test section two speakers (JBL 2206H) are mounted over the holes, one on each side of the test section. The loudspeakers are not fixed to the test section but mounted on an independent rigid frame. The slit between the test section wall and the rim of the loud speaker is filled with a 5 mm thick rim of closed-cell foam. This provides an acoustical seal with a minimum of mechanical contact. The speakers are connected in series and out of phase, such that both membranes have displacements in the same direction with respect to each other. The speakers are driven by an amplifier (QSC RMX2450) which in turn is driven by a function generator (Yokogawa FG120). In both side walls of the test section piezoelectric pressure transducers (PCB 116A and Kistler 7031) are mounted at a distance of 149 mm upstream of the leading edge of the airfoil. The transducers are positioned in order to measure the acoustic field. The piezoelectric transducers are mounted on a 1 cm thick layer of closed-cell foam, which is glued to the wall of the test section. They have been mounted such that there is no direct mechanical contact with the wall. The eigenfrequency of the microphone with foam suspension is tuned to be significantly below the frequency at which the speakers are driven. This isolates the microphones from wall vibrations. In the middle of the test section a NACA0018 profile is mounted vertically. The airfoil is manufactured out of extruded aluminium and approximates the NACA0018 profile definition within an accuracy of 0.2 mm.<sup>8</sup> In the experiments two airfoils are used, a standard NACA0018 profile and a standard NACA0018 profile with a cavity. The chord  $c$  of both airfoils is 165 mm and the width is 495 mm such that it spans the entire test section from top to bottom, closing tightly at the ends. The geometry of the NACA0018 profile with the location of the pressure transducers is shown in figure 2. More details on the airfoil with cavity are given in section V. The vertical positioning of the airfoil provides practical advantages related to the placement of experimental equipment. The bottom of the airfoil is fixed by a pin-in-hole connection. The top is connected by a tube to a flange which is bolted to the test section. This allows for modification of the angle of attack of the airfoil, which can be set with an accuracy of 0.5 deg. At an angle of attack of zero degrees the blockage in the test section is 2%.

In the airfoil two miniature dynamic pressure transducers (Kulite XCS-093-140mBarD) are placed flush to the surface, on either side of the airfoil at a position of 13.3% of the chord measured from the leading edge. This location has been chosen because the pressure fluctuations are expected to be highest there. The part of the airfoil containing the pressure transducers has been sealed air tight, except for the circular tube which sticks out of the wind tunnel. A sketch of the test section is given in figure 1.

All signals from the pressure transducers and the signal from the signal generator are recorded with a National Instruments data acquisition system (NI SCXI-1000). The unsteady data is processed using a lock-in method, which allows the extraction of the component of the pressure signal at the excitation frequency and determine its phase. The phase is determined with respect to the acoustic pressure measured by means of the piezoelectric-electrical transducers placed in the side walls. The signal from the function generator is used as the reference signal for the lock-in method. A Hilbert transform is used to obtain a complex harmonic function from the reference signal.

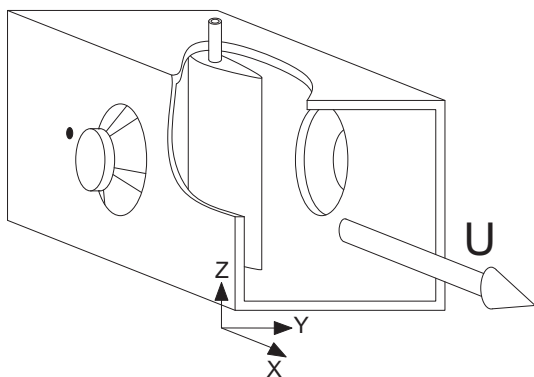


Figure 1. Sketch of the test section of the wind tunnel with speakers mounted and the airfoil placed in the middle. One of the pressure transducers in the wall is visible just in front of the left speaker.

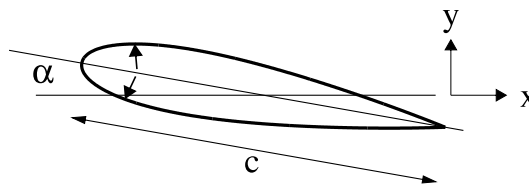


Figure 2. Standard NACA0018 profile with chord  $c$ . The location of the pressure transducers is indicated by the arrows inside the profile. The angle of attack is defined positive as indicated in the figure.

The signal generator is tuned to the first transversal eigenfrequency ( $f = 331$  Hz) of the wind tunnel with the wing installed, creating a transversal standing wave. The result is equivalent to moving the airfoil vertically in a steady uniform flow. Typically the non-dimensional amplitude of the velocity oscillation at

the centre of the wind tunnel is in the order of  $v'/U_\infty = O(10^{-2})$ . Here  $v'$  denotes the amplitude of the velocity fluctuation, where the prime indicates an acoustic velocity, and  $U_\infty$  is the free stream velocity.

The value of the Strouhal number can be varied by adjusting the free stream velocity. For the current setup Strouhal numbers down to a value of 2.5 can be obtained. In the experiments the Reynolds number varies from  $2 \cdot 10^5$  to  $7 \cdot 10^5$ .

### III. Numerical and analytical model

The numerical method used in this paper is a two-dimensional Euler code for internal flows, an Euler code for internal acoustics (EIA).<sup>9</sup> The numerical method is based on a second-order accurate finite-volume spatial discretization in the interior and a finite-difference discretization of the compatibility relations on the boundary. The Euler equations are integrated in time using a multistage Runge-Kutta explicit time stepping scheme. Numerical dissipation in the code ensures that the Kutta condition is fulfilled at sharp edges. The structured grid is generated with the build-in algebraic grid generator of EIA. In the numerical simulations the test section of the wind tunnel is modelled as a duct segment of 2.5 m, the speakers are modelled as flush mounted moving pistons in the side walls. At the inlet and outlet of the duct anechoic boundary conditions are applied. For the case of the standard NACA0018 profile a structured grid of 16 blocks is constructed, with an embedded C grid around the profile. The total number of cells for this grid is about 4000. For the NACA0018 profile with cavity a structured grid of 28 blocks is generated with an embedded C grid around the profile and another embedded C grid to mesh the cavity. The total number of cells in this grid is about 4500.

For the case of a flat plate oscillating in a uniform, two-dimensional, and incompressible flow with velocity  $U_\infty$  an analytic solution can be found using linear potential theory.<sup>2</sup> In this paper this model will be referred to as Theodorsen's theory. A Joukowski mapping is used to transform the flat plate in the physical plane into a circle in the transformed plane. The coordinate along the circle in the transformed plane, which corresponds to the plate in the physical plane, is denoted by  $\theta$ . If the plate stretches from  $x = -1$  to  $x = 1$ ,  $x = \cos \theta$ . It can be shown that the pressure difference over the plate at a certain location  $\theta$  is equal to

$$\Delta p_u = -2\hat{v}\rho_\infty U_\infty \left[ C(k_b) \tan \frac{\theta}{2} + ik_b \sin \theta \right] \quad (1)$$

where  $\hat{v}$  is the amplitude of the velocity fluctuation of the plate in the direction normal to the main flow,  $k_b$  is the Strouhal number and  $C(k_b)$  is known as the Theodorsen function. It is the quotient of modified Bessel functions of the second kind of order zero and order one. The subscript  $u$  emphasizes that this is in an unsteady flow. The results of the measurements will be presented by the non-dimensional pressure difference  $\Delta C_{p_u}$ . For the theoretical model for a flat plate, where the plate is fixed in an oscillating flow instead of the other way round, this non-dimensional pressure difference can be shown to be equal to

$$\Delta C_{p_u} = \frac{\Delta p_u}{\frac{1}{2}\rho_\infty U_\infty v'} \quad (2)$$

Where the  $\hat{v}$  is replaced by  $v'$  to indicate that we are now dealing with an acoustic velocity rather than the velocity of the plate. The results of the theory and the measurements will be presented in the frequency domain, i.e., in terms of amplitude and a phase.

### IV. Validation

In order to validate the experimental procedure a standard NACA0018 airfoil is mounted in the wind tunnel. Both steady and unsteady measurements are performed and compared to the results of potential theory for a flat plate and the results of Euler simulations. In the Euler simulations the entire test section of the wind tunnel is modelled, including the airfoil.

#### IV.A. Steady flow

We first consider the case with no acoustic forcing, so there is only a main flow in the test section with velocity  $U_\infty$ . The pressure difference at 13.3% of the chord length from the leading edge is measured

for several angles of attack  $\alpha$  and is plotted in figure 3. The results are presented as a difference in the pressure coefficient,  $\Delta C_p$ , between the upper and lower side of the airfoil  $\Delta C_p = \frac{2(p_{lower} - p_{upper})}{\rho_{\infty} U_{\infty}^2}$ . The angle of attack  $\alpha$  is defined positive nose-up, see figure 2. Figure 3 shows that the measurements of the non-

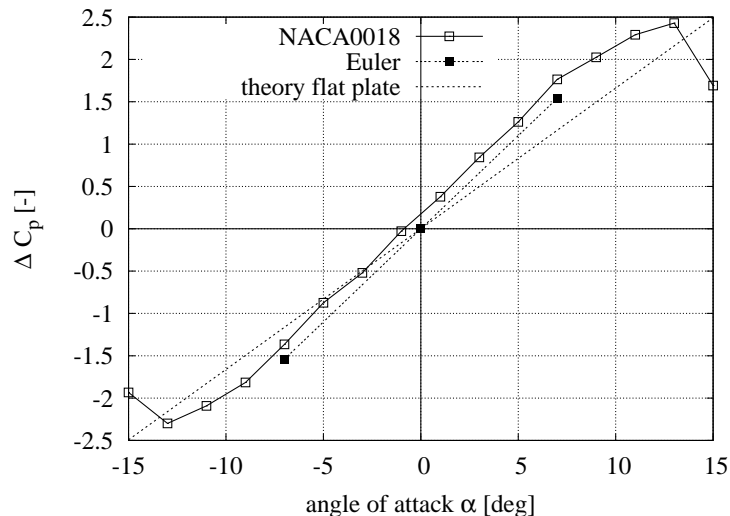


**Figure 3.** Non-dimensional pressure difference  $\Delta C_p$  over the airfoil at 13.3% of the chord from the leading edge as a function of the angle of attack for a standard NACA0018 airfoil (solid line with open square markers). Also shown are the results for a flat plate (broken line) and the results of numerical Euler simulations (broken line with solid square markers).

dimensional pressure difference at 13.3% chord length from the leading edge are 20% higher compared to the results of classical potential theory for a flat plate. For small angles of attack the measurements agree well with the results of Euler simulations, which indicates that the difference between flat-plate theory and the measurements on the NACA0018 airfoil are due to the thickness of the profile and the effect of the wind tunnel walls, which is not taken into account by classical potential theory for a flat plate. Around  $\alpha = 10^\circ$  the measurements on the standard airfoil start to deviate from the results of the Euler simulations, which is an indication that the flow is separated. The theoretical results are symmetric with respect to the origin, which is to be expected with a symmetric airfoil. We observe a small deviation in the measured results, which can be due to a systematic error of about 1 degree in the angle of attack.

#### IV.B. Unsteady flow

For the unsteady flow case, the speakers are tuned to the first transversal resonance frequency ( $f=331$  Hz) of the wind tunnel with wing installed. The angle of attack of the standard NACA0018 profile is set to zero degrees. The measurements have been performed for several values of the Strouhal number by varying the freestream velocity  $U$ .

The results are presented in terms of non-dimensional pressure differences, but now the unsteadiness of the flow is also taken into account. This is done by defining an unsteady non-dimensional difference in pressure coefficient  $\Delta C_{p_u}$  as discussed in section III. The results are presented in the frequency domain, as a function of the Strouhal number. The phase is determined with respect to the transversal acoustic velocity fluctuations at the centre of the wind tunnel. This transversal velocity is determined at a distance of 149 mm upstream of the airfoil, from the amplitude of the acoustic pressure measured at the wall of the wind tunnel, see figure 1. The amplitude of the pressure difference is plotted in figure 4 as a function of the Strouhal number and the corresponding phase is shown in figure 5. In figure 4 it is seen that there is an offset of the amplitude with respect to Theodorsen's theory. Figure 5 shows that the phase of the measurements is consistently above the phase predicted by Theodorsen's theory and agree with the phase obtained from the numerical Euler simulations.

The measurements of the non-dimensional difference in pressure coefficient have been repeated for different excitation amplitudes and different values of the angle of attack, ranging from -5 to +5 degrees. The results are reproducible and all of the measurements are within a few percent of the measurements presented above. Based on Theodorsen's theory one would expect to see no influence of the amplitude or angle of

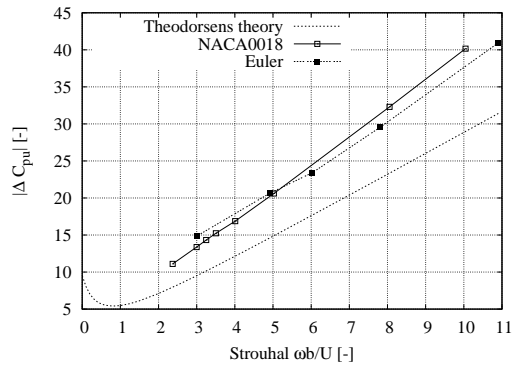


Figure 4. Amplitude of dynamical non-dimensional pressure difference over NACA0018 airfoil (solid line with open square markers), Theodorsen's theory (broken line) and the results of Euler simulations (broken line with solid square markers). For an amplitude of about  $v'/U_\infty=0.5\%$ .

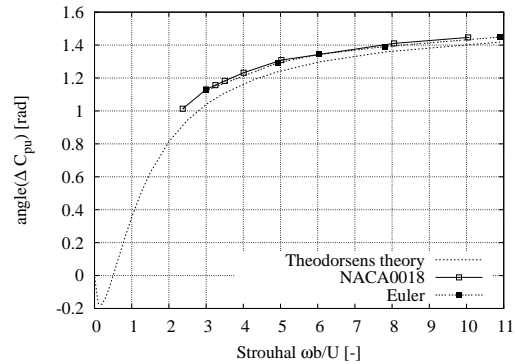


Figure 5. Phase of dynamical non-dimensional pressure difference over NACA0018 airfoil (solid line with open square markers), Theodorsen's theory (broken line) and the results of Euler simulations (broken line with solid square markers). The phase is determined with respect to the velocity fluctuations  $v'$ . For an amplitude of about  $v'/U_\infty=0.5\%$ .

attack, as long as both the angle of attack and amplitude are small.

## V. Influence of the cavity in steady flow

In this section the results of static pressure measurements for various angles of attack are presented for the NACA0018 airfoil with cavity. The results of the airfoil with cavity are compared to the measurements of the standard NACA0018 airfoil without cavity and numerical results of the Euler code.

The chord  $c = 2b$  of the airfoil is 165 mm and the width  $W$  of the cavity is 34 mm, as shown in figure 6. The distance from the trailing edge to the rear edge of the cavity is 97 mm. The edges of the cavity are sharp and the upper side is defined as the side with the cavity. This specific cavity was inspired by the shape of the cavity designed within the European project VortexCell2050. It is optimized for minimal production time and production cost; it has not yet been optimized to trap a vortex. In figure 7 the results for the standard NACA0018 airfoil and the NACA0018 airfoil with cavity are indicated by the solid line with square markers and the broken line with circular markers, respectively. The results of the Euler simulations are indicated by the broken line with solid circular markers. The results of the time average of the difference in pressure coefficients in an unsteady flow, where acoustic forcing is present, have also been determined. The results are right on top of the steady measurements shown in the figure by the dotted line with circular markers and have therefore been omitted in figure 7. As before, the angle of attack is defined positive nose-up. It is evident that there is an asymmetry compared to the standard airfoil. Especially for negative angles of attack a significant discrepancy in  $\Delta C_p$  is present between the standard airfoil and the airfoil with cavity. The numerical Euler code is unable to predict the local non-dimensional pressure difference correctly. In the numerical simulations a periodic vortex shedding is observed. The experimentally measured pressure does not show the unsteady behaviour observed in the numerical simulation upon vortex shedding. It is also clear that the acoustic forcing has no effect on the mean pressure difference over the airfoil. The difference between experiment and numerical simulations could be due to the three-dimensional character of the actual flow in contrast with the two-dimensional simulations, or due to viscous effects.

## VI. Influence of the cavity in unsteady flow

The results of dynamic pressure measurements on the NACA0018 airfoil with a cavity will be presented in this section. The results will be compared to the measurements of the standard NACA0018 airfoil and numerical Euler simulations of the airfoil with cavity. Again the results will be presented as non-dimensional pressure differences as a function of the Strouhal number. In general the separation from the front edge of the cavity is three-dimensional. However, it is known that if there is a periodic disturbance of a high enough amplitude this will cause the separation to synchronize along the spanwise direction and will cause the flow to behave as a quasi-two-dimensional flow.

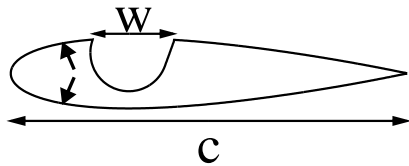


Figure 6. NACA0018 airfoil, with chord  $c$  and cavity with width  $W$ . The location of the pressure transducers is indicated by the arrows inside the profile.

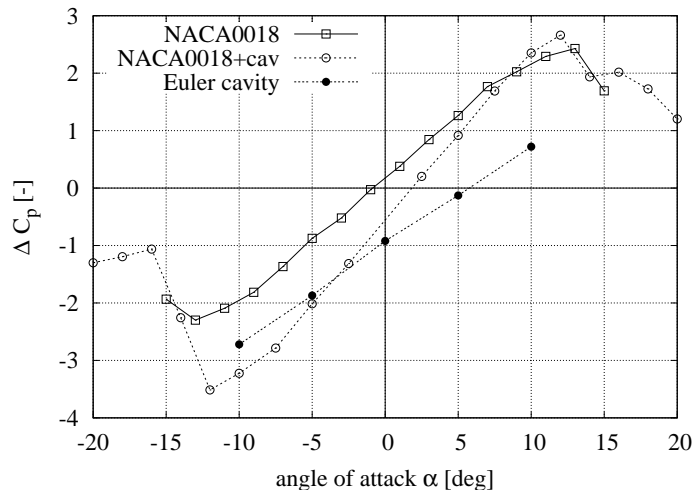


Figure 7. Non-dimensional pressure difference between upper and lower side of a standard NACA0018 airfoil (solid line with open squares) the NACA0018 airfoil with cavity (broken line with open circular markers) and numerical results of 2D Euler simulations for the airfoil with cavity (broken line with solid circular markers), versus angle of attack.

Figure 8 and figure 9 display the results of measurements performed on the NACA0018 airfoil with cavity at an angle of attack of zero degrees. On the vertical axis in figure 8 the amplitude of the non-dimensional pressure difference is shown, while on the horizontal axis the value of the Strouhal number is plotted. Figure 9 shows the corresponding phase. Figure 8 shows a slight deviation of  $|\Delta C_{pu}|$  around a  $k_b = 3.0$  compared to

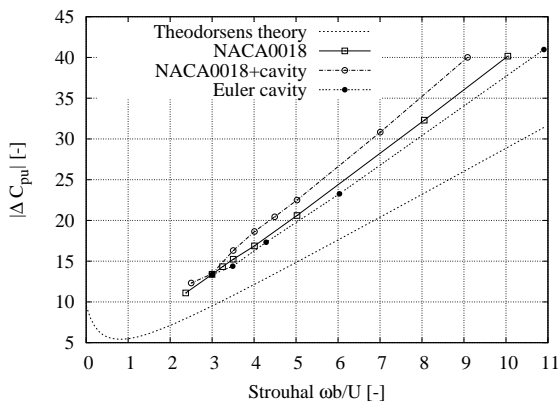


Figure 8. Amplitude of dynamical non-dimensional pressure difference over a standard NACA0018 airfoil (solid line with open squares), the NACA0018 airfoil with cavity (broken line with open circular markers), the results of the Euler simulations of the airfoil with cavity (broken line with solid circular markers) and Theodorsen's theory (broken line).

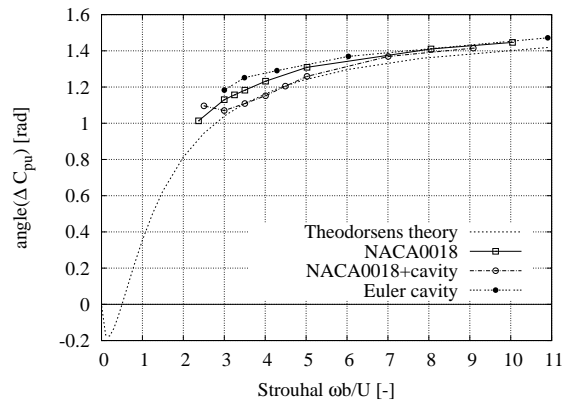


Figure 9. Phase of dynamical non-dimensional pressure difference over a standard NACA0018 airfoil (solid line with open square markers), measurements on the NACA0018 airfoil with cavity (broken line with open circular markers), the results of the Euler simulations (broken line with solid circular markers) and Theodorsen's theory (broken line). The phase is determined with respect to the velocity fluctuations  $v'$ .

the standard NACA0018 airfoil. Also the amplitude of the difference in pressure coefficient seems to increase faster with increasing Strouhal number above  $k_b = 3.5$  compared to the standard NACA0018 airfoil, i.e. the slope is steeper. The Euler code seems unable to predict the increased value of  $\Delta C_{pu}$  with respect to the standard airfoil. Figure 9 shows that the phase of the NACA0018 airfoil with cavity deviates slightly from the standard airfoil around  $k_b = 3.0$ . The Euler simulations show a phase which is consistently above the phase predicted by Theodorsen's theory and appears to be higher than the Euler code predicted for the standard NACA0018 airfoil.

## VII. Conclusion

The influence of a cavity, in a NACA0018 airfoil on the local pressure difference measured just downstream of the leading edge was investigated. It has been demonstrated that the cavity influences the local pressure difference over the airfoil in a steady flow. Here the main effect of the cavity is to cause an asymmetry between the pressure coefficient at a positive and a negative angle of attack. In an oscillating flow the airfoil with cavity shows only minor deviations with respect to the oscillating pressure difference over a standard NACA0018 airfoil. Above  $k_b = 3.5$  the amplitude of the non-dimensional pressure difference of the airfoil with cavity is higher than that of the standard airfoil.

The two-dimensional Euler code was unable to predict the effect of the cavity on the pressure coefficient in a steady flow. However, in both a steady flow and an oscillating unsteady flow the agreement between the measurements on the standard NACA0018 airfoil and Euler simulations was good.

Since only local pressures were measured, it is not possible to provide information about the lift and drag, until a numerical model is able to reproduce the experimental data.

## Acknowledgments

The authors wish to acknowledge A. Holten, F. van Uittert and G. Oerlemans for technical support. Further we would like to thank I. Lopez and G.J.F. van Heijst for fruitful discussions and suggestions.

## References

- <sup>1</sup>[www.vortexcell2050.org](http://www.vortexcell2050.org)
- <sup>2</sup>Fung, Y.C., *An Introduction to the Theory of Aeroelasticity*, 1965.
- <sup>3</sup>Dowell, E.H., *A Modern Course in Aeroelasticity*, 2004.
- <sup>4</sup>Halfman, R.L., *Experimental Aerodynamic Derivatives of a Sinusoidally Oscillating Airfoil in Two-Dimensional Flow* NACA Rept. 1108, 1952.
- <sup>5</sup>Schewe, G., Mai, H., Dietz, G., *Nonlinear effects in transonic flutter with emphasis on manifestation of limit cycle oscillations*, Journal of Fluids and Structures, 18, 2003, pp. 3-22.
- <sup>6</sup>Rockwell, D., and Naudasher E., *Self-sustained oscillations of flow past cavities*, Trans. ASME: J. Fluid Eng. 100, 1978, pp. 152-165.
- <sup>7</sup>Gharib, M., Roshko, A., *The effect of flow oscillations on cavity drag*, J. Fluid Mech. 177, 1987, pp.501-530.
- <sup>8</sup>Private comm. Chris Boeije, Engineering Fluid Dynamics, Twente University, 2008.
- <sup>9</sup>Hulshoff, S.J., *EIA: an Euler Code for Internal Acoustics. Part 1: Method description and User's Guide*, Tech. Rept., Eindhoven University of Technology, 2000.